

# Higgs Boson Properties and BSM Higgs Boson Searches at LHC

W. F. Mader (on behalf of the ATLAS and CMS collaborations)  
Technical University Dresden, 01062 Dresden, Germany

At the end of 2008, the Large Hadron Collider (LHC) will come into operation and the two experiments ATLAS and CMS will start taking data from proton-proton collisions at a center-of-mass energy of  $\sqrt{s} = 14$  TeV. In preparation for the data taking period, the discovery potential for Higgs bosons beyond the Standard Model has been updated by both experiments and is reviewed here. In addition, the prospects for measuring the properties of a Higgs boson like its mass and width, its CP eigenvalues and its couplings to fermions and gauge bosons are discussed.

## 1. MSSM HIGGS BOSON SEARCHES

In the Minimal Supersymmetric Standard Model (MSSM), the minimal extension of the Standard Model (SM), two Higgs doublets are required, resulting in five observable Higgs bosons. Three of them are electrically neutral ( $h$ ,  $H$ , and  $A$ ) while two of them are charged ( $H^\pm$ ). At tree level their properties like masses, widths and branching fractions can be predicted in terms of only two parameters, typically chosen to be the mass of the CP-odd Higgs boson,  $m_A$ , and the ratio of the vacuum expectation values of the two Higgs doublets,  $\tan\beta$ .

In the MSSM the couplings of the Higgs bosons to fermions and bosons are different from those in the Standard Model resulting in different production cross-sections and decay rates. The coupling of the Higgs bosons to third generation fermions is strongly enhanced for large regions of the parameter space which determines the search strategies for such Higgs bosons.

In the following, searches for the neutral and charged Higgs bosons in the MSSM in the two experiments ATLAS and CMS at the LHC are described. Unless indicated otherwise, all results will be given in the  $m_h^{\max}$  scenario [1]. A detailed description of the ATLAS and CMS detectors can be found elsewhere [2, 3]

### 1.1. Higgs Boson Searches in $h/H/A \rightarrow \mu\mu$

In the SM the discovery potential for the Higgs boson in the dimuon final state is limited due to its small branching fraction and the high backgrounds expected from several SM processes. However, in the MSSM the decay of the three neutral Higgs bosons  $h$ ,  $H$ , and  $A$  into a dimuon final state can be strongly enhanced depending on the value of  $\tan\beta$ . This channel can therefore serve as a discovery channel for high values of  $\tan\beta$ , or as a tool to exclude large parts of the  $m_A$  vs.  $\tan\beta$  plane. In addition, in the intense coupling region around  $m_A = 130$  GeV where all the neutral Higgs bosons have a comparable mass, the excellent invariant mass resolution of the dimuon final state offers the potential to observe these states individually at the same time.

The event selection is optimized separately for the cases where zero or at least one  $b$  jet are identified in the final state. In the first case Drell-Yan  $Z$  boson production is the dominant background, while in the second case the dominant contribution is approximately equally shared between the  $Z$  and  $t\bar{t}$  processes. At the preselection step two isolated muons of opposite charge are required inside the acceptance region with a  $p_T > 20$  GeV. Due to the high momenta of the muons from the Higgs boson decays this final state can be efficiently triggered by a high- $p_T$  single-muon trigger. Further selection criteria include an upper cut on the amount of missing energy found in the event, requirements on the jet identified as coming from a  $b$  quark (or a  $b$ -jet veto in the case of the zero  $b$ -jet analysis), on the acoplanarity of the dimuon system and the sum of  $p_T$  of all jets in the event (in the case of the one  $b$ -jet analysis).

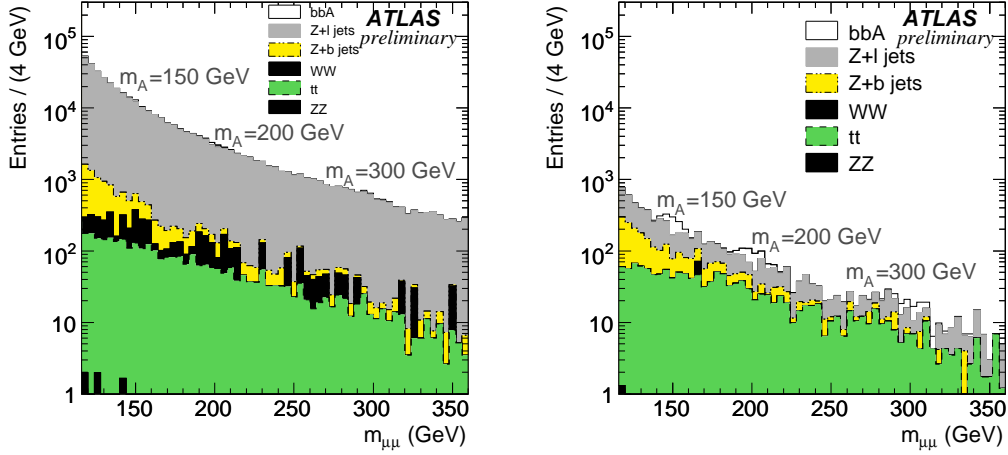


Figure 1: Invariant dimuon mass distribution of the main backgrounds and the  $A$  boson signal at masses  $m_A = 150, 200,$  and  $300$  GeV and  $\tan\beta = 30$ , obtained for an integrated luminosity of  $30\text{ fb}^{-1}$  in ATLAS.  $B$ -tagging has been applied for the event selection. The production rates of  $H$  and  $A$  bosons have been added. Zero or at least one  $b$ -jet have been required in the left-hand side and the right-hand side plot, respectively.

The invariant dimuon mass after all selection criteria is displayed for the cases of zero and at least one  $b$ -jet on the left-hand side and the right-hand side of Figure 1, respectively. The background from  $Z$  and  $t\bar{t}$  events is estimated from data. The  $Z$  background is estimated from data by analyzing the  $ee$  final state which is signal-free. In the case of  $t\bar{t}$  events, the  $e\mu$  final state or a  $t\bar{t}$  enriched sample obtained by requiring large missing  $E_T$  in the event can be used.

The discovery potential as obtained by CMS and ATLAS is displayed on the left-hand side and the right-hand side of Figure 2, respectively [4, 5]. The theoretical uncertainties include the uncertainty on the parton density functions and on the renormalization and factorization scales. The dominant experimental uncertainties (of about 10% in total) include the reconstruction efficiency, momentum resolution and momentum scale for the muons, the jet energy scale and resolution as well as the uncertainty on the  $b$  tagging efficiency and the light-jet rejection rate.

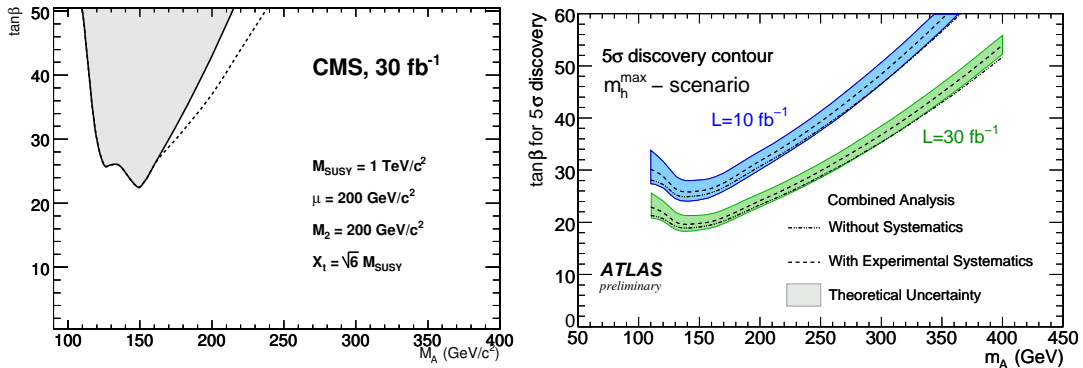


Figure 2: Discovery potential in the  $h/H/A \rightarrow \mu\mu$  channel as a function of  $m_A$  and  $\tan\beta$ . Left: Discovery potential from CMS for an integrated luminosity of  $30\text{ fb}^{-1}$ . In the shaded area  $> 5\sigma$  significance can be obtained; the dashed line corresponds to the  $5\sigma$  contour without systematic uncertainties included. Right: The  $5\sigma$  discovery contours from ATLAS corresponding to integrated luminosities of  $10$  and  $30\text{ fb}^{-1}$  with (dashed line) and without (dotted line) systematic uncertainties taken into account. The theoretical uncertainties are illustrated by the shaded bands.

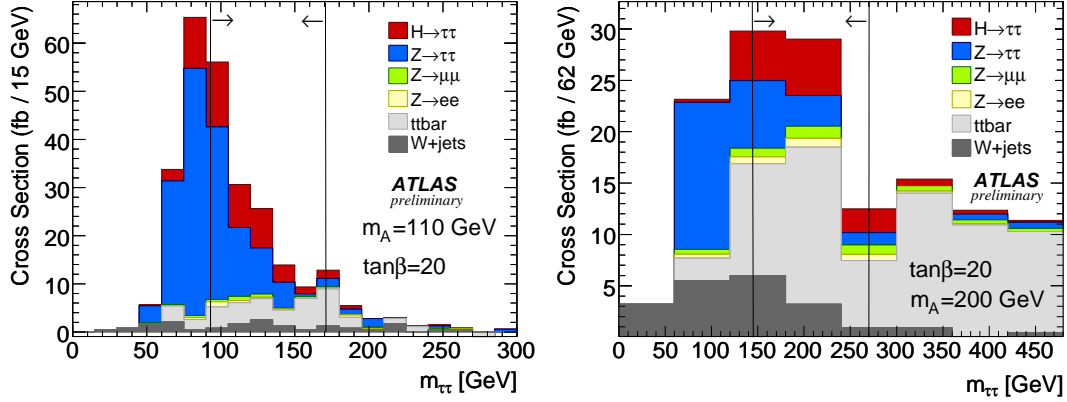


Figure 3: Invariant  $m_{\tau\tau}$  distribution for signal and background events. The distributions are shown after all selection cuts for Higgs bosons masses and  $\tan\beta$  values as indicated in the plots. The vertical lines indicate the mass window used for calculating the signal significance.

## 1.2. Higgs Boson Searches in $h/H/A \rightarrow \tau\tau$

Compared to the dimuon final state,  $h/H/A \rightarrow \tau\tau$  decays have a substantially larger branching fraction which scales as  $(m_\tau/m_\mu)^2$  for a given  $\tan\beta$ . However, since the  $\tau$  leptons can decay both, leptonically and hadronically, the signatures observed in the detector are very different and therefore have to be treated individually.

### 1.2.1. Higgs Boson Searches in $h/H/A \rightarrow \tau\tau \rightarrow \ell\ell\nu$

Even though the branching fraction of the two  $\tau$  leptons into a fully leptonic final state is only 12%, it contributes significantly to the discovery potential in particular for Higgs boson masses in the range  $110 < m_A < 300$  GeV. These events can be triggered on with high efficiency using an electron and/or muon trigger.

The event topology consists of two leptons, missing  $E_T$ , and jets. The main background is coming from Drell-Yan  $\tau\tau$  production,  $t\bar{t}$  processes, and  $W$ +jets topologies. The CMS analysis only studies the  $e\mu$  final state [6] while ATLAS exploits all leptonic final states [5]. The invariant di- $\tau$  mass is reconstructed using the collinear approximation technique [7].

In Figure 3 the invariant di- $\tau$  mass distribution as obtained in ATLAS is shown for Higgs boson masses of  $m_A = 110$  GeV, and  $m_A = 200$  GeV,  $\tan\beta = 20$  and an integrated luminosity of  $30\text{fb}^{-1}$ . For low masses, the irreducible  $Z \rightarrow \tau\tau$  background dominates over that from  $t\bar{t}$  processes, while for high masses the situation is reversed. The dominant experimental systematic uncertainties come from the jet-energy scale and resolution uncertainty and from the uncertainty on the  $b$ -tagging efficiency. The theoretical uncertainties come from the uncertainties on the parton density functions, on the factorization and renormalization scale for signal and  $t\bar{t}$  background.

The discovery potential for this channel is shown in Figure 4 for ATLAS (left) and CMS (right). For low Higgs boson masses of the order of 130 GeV, a discovery with at least  $5\sigma$  significance will be possible for  $\tan\beta$  values of 15 or larger, while for higher Higgs boson masses like  $m_A = 200$  GeV  $\tan\beta$  of the order of 30 would be necessary.

### 1.2.2. Higgs Boson Searches in $h/H/A \rightarrow \tau\tau \rightarrow \ell h3\nu$

The lepton-hadron final state consists of one electron or muon plus jets, one of which is identified as coming from a hadronically decaying  $\tau$  lepton, and missing energy in the event. A single electron or muon trigger, either standalone or combined with a  $\tau$  trigger, is used to preselect the events. One jet in the event is required to be identified as coming from a  $b$  quark in order to suppress backgrounds from Drell-Yan  $\tau\tau$  production, from QCD multi-jet events and from  $W$ +jet backgrounds. Details of the analyses can be found in [8, 9].

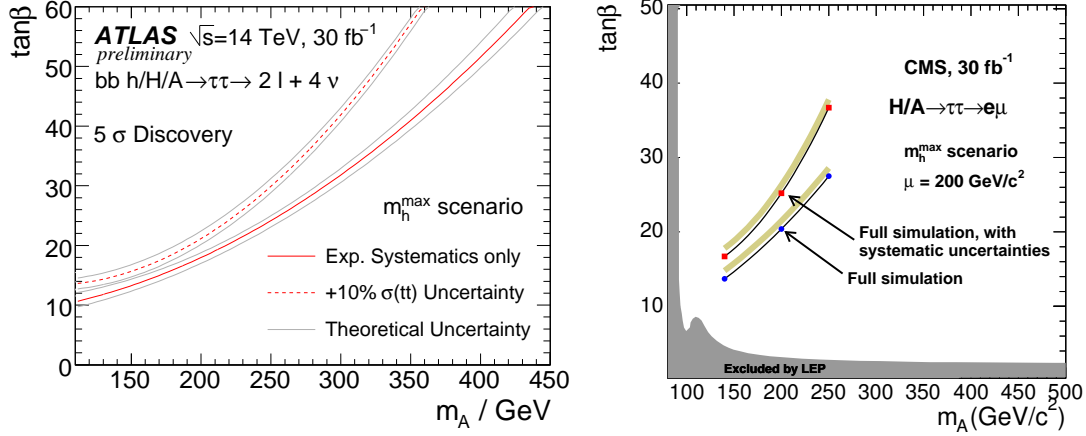


Figure 4: The  $5\sigma$  discovery contours in the  $m_A$  vs.  $\tan\beta$  plane for the fully leptonic final state and for an integrated luminosity of  $30\text{ fb}^{-1}$  with systematic uncertainties taken into account for ATLAS (left) and CMS (right).

The invariant  $\tau\tau$  mass is reconstructed using the collinear approximation technique, and is displayed in Figure 5 for the  $\mu + \tau$ -jet (left) and  $e + \tau$ -jet (right) final state, respectively.

For the  $\mu + \tau$ -jet final state the main background after all selection cuts is represented by  $\tau\tau b\bar{b}$ , Drell-Yan  $Z \rightarrow \tau\tau$ , and  $t\bar{t}$  processes. The  $t\bar{t}$  background is estimated from data by inversion of the electron veto cut and has a systematic uncertainty of 12.4%. The Drell-Yan  $\tau\tau$  prediction is taken from a high precision measurement assumed to be done at the time of this analysis and a total systematic uncertainty of 8% is assigned. Finally, the  $b\bar{b}\tau\tau$  background is assumed to be known with a systematic uncertainty of 15%, derived from the uncertainty on a  $\mu\mu b\bar{b}$  cross section measurement and from the jet-energy scale uncertainty.

For the  $e + \tau$ -jet analysis the main background comes from  $(b\bar{b})Z/\gamma^* \rightarrow ee/\tau\tau$  final states and from  $t\bar{t}$  processes. The total systematic uncertainty was calculated from the background uncertainties (either measured or predicted from theory) and the experimental uncertainties of the event selection, like electron and  $\tau$  identification, calorimetric energy scale and  $b$  tagging efficiency.

The discovery potential for the  $\mu + \tau$ -jet and the  $e + \tau$ -jet analysis is displayed in Figure 6 on the left-hand side and the right-hand side, respectively. The discovery of a Higgs boson with a mass of the order of  $m_A = 200$  GeV would be possible even for low  $\tan\beta$  values, while for high masses such a discovery would be challenging.

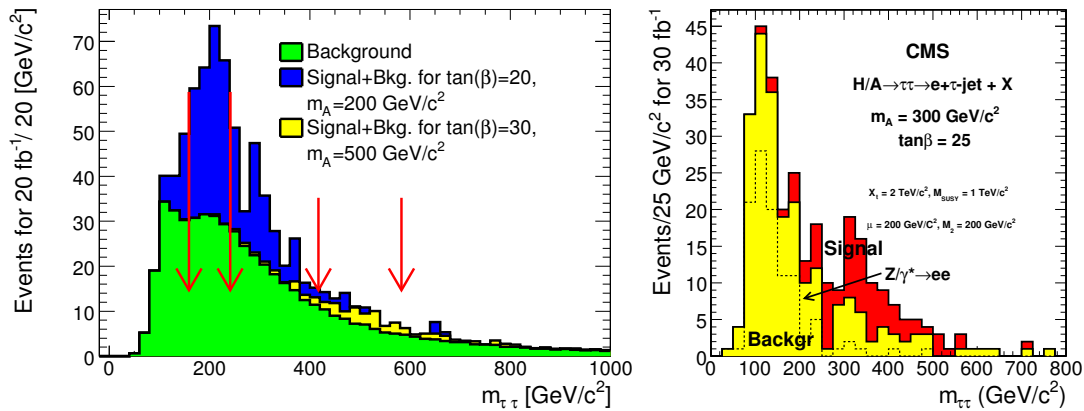


Figure 5: Invariant  $m_{\tau\tau}$  distribution for the  $\mu + \tau$ jet +  $X$  (left) and the  $e + \tau$ jet +  $X$  (right) final state for Higgs boson masses,  $\tan\beta$  values as indicated in the plots, and for an integrated luminosity of  $30\text{ fb}^{-1}$ . In the left plot, the mass windows in which the numbers of events are counted for the significance calculation are indicated by the vertical arrows.

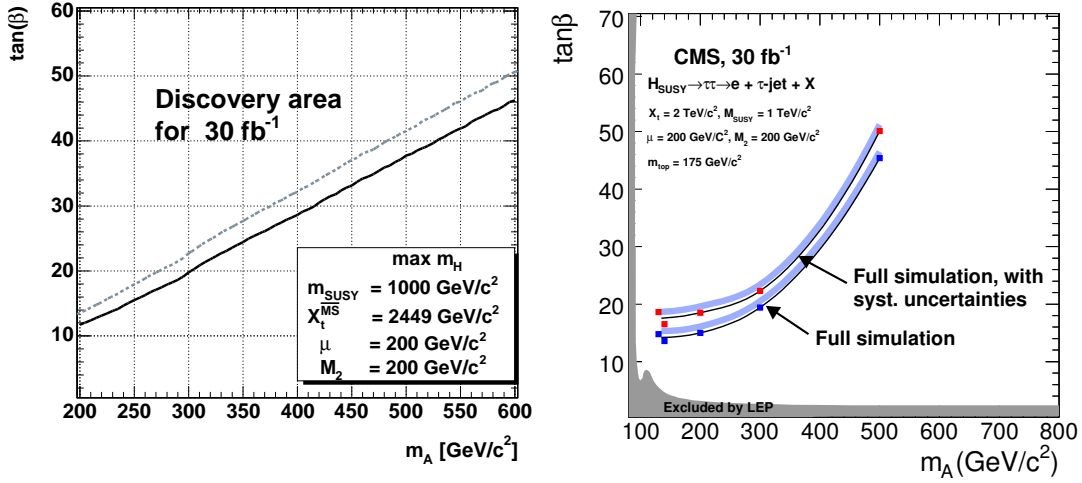


Figure 6: The  $5\sigma$  discovery contours in the  $m_A$  vs.  $\tan\beta$  plane and for an integrated luminosity of  $30\text{fb}^{-1}$ . Left: Discovery contour for the  $\mu + \tau\text{jet} + X$  final state, with (dashed) and without (solid) the systematic uncertainties on the background taken into account. Right: Discovery contour for the  $e + \tau\text{jet} + X$  final state, with and without the systematic uncertainties taken into account as indicated in the plot. The exclusion limit as obtained from LEP is indicated by the shaded area.

### 1.2.3. Higgs Boson Searches in $h/H/A \rightarrow \tau\tau \rightarrow hh2\nu$

This analysis has been performed for Higgs bosons of mass 200, 500, and 800 GeV. The observed final state consists of two  $\tau$ -like jets identified by their high transverse energy and a  $p_T > 30$  GeV for the leading track inside the  $\tau$ -jet. Furthermore, exactly one additional jet with  $E_T > 20$  GeV was allowed. This jet had to pass the tagging criteria for a  $b$ -jet based on 3D-impact parameters. Details of the analysis can be found in [10].

After all selection criteria, the dominant background comes from QCD multi-jet events. In order to estimate this background from Monte Carlo, the selection has been factorized into three categories: Trigger and offline calorimetric reconstruction,  $\tau$  identification, and finally jet reconstruction,  $b$ -tagging and  $m_{\tau\tau}$  mass reconstruction.

The invariant  $m_{\tau\tau}$  mass distribution for two Higgs boson masses ( $m_A = 200$  and  $600$  GeV) and for an integrated luminosity of  $60\text{fb}^{-1}$  are displayed in Figure 7. The systematic uncertainties considered are from the  $E_T^{\text{miss}}$  and jet energy scale (3 – 10%), tracker misalignment ( $\sim 10\%$ ), and the measurement of the QCD background from data (5 – 20%). Including all systematic uncertainties, a  $5\sigma$  discovery for a Higgs boson of mass  $m_A = 200/500/800$  GeV can be achieved for a  $\tan\beta$  value of 21/34/49.

## 1.3. Searches for the Charged Higgs Boson

The discovery of a charged Higgs boson would be a definite signal for the existence of new physics beyond the SM. It is predicted in many non-minimal Higgs scenarios like Two Higgs Doublet Models (2HDM) or models with Higgs triplets. The search strategies for a charged Higgs boson depend on its mass which determines the production rate as well as the available decay modes. Below the top quark mass, the main production mode is through top quark decays ( $t \rightarrow H^+b$ ) and the decay of the charged Higgs boson proceeds predominantly via the  $H^+ \rightarrow \tau\nu$  process. Above the top quark threshold, the production processes are  $gg \rightarrow tbH^+$  and  $gb \rightarrow tH^+$ , where the latter dominates. The decay proceeds predominantly via the  $tb$  final state.

Charged Higgs boson searches involve several higher level reconstructed physics objects such as electrons, muons, jets, jets tagged as  $b$  jets and jets identified as  $\tau$  jets. The trigger to select the relevant event topologies consists of a combination of  $\tau$  triggers,  $E_T^{\text{miss}}$  triggers, and jet triggers. Details on the analyses can be found in References [5? ].

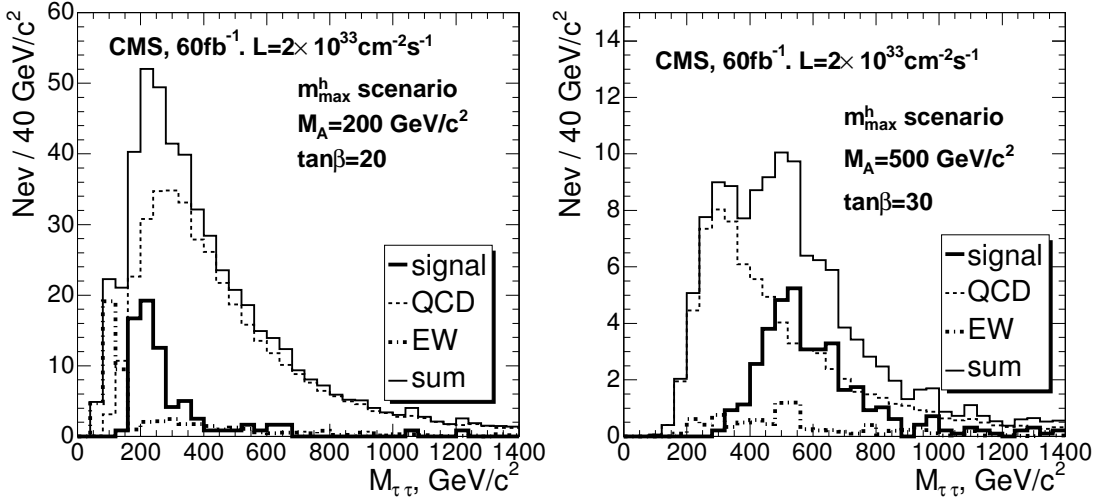


Figure 7: The  $m_{\tau\tau}$  distributions for a signal of  $m_A = 200$  GeV with  $\tan\beta = 20$  (left), for  $m_A = 500$  GeV with  $\tan\beta = 30$  (right), and for the background in  $60 \text{ fb}^{-1}$  of data. The solid histogram represents the distribution expected from all candidates which is composed of the signal (thick solid line), QCD background (dashed line), and irreducible background (thick dashed-dotted line).

### 1.3.1. Light Charged Higgs Boson Searches: $m_{H^\pm} < m_t$

If the charged Higgs boson is light, the branching fraction of the top quark into a  $bW$  final state might be less than that predicted by the SM. In that case the expected background from SM-like  $t\bar{t}$  decays is reduced which has to be taken into account.

Three different channels have been analyzed, classified according to the final state of the  $\tau$  and  $W$  decays:

- $b\tau(\text{had})\nu bW(\text{had})$ : This channel has a high branching fraction which makes it a priori one of the most important discovery channels. However, the absence of leptons and the high hadronic activity makes this channel particularly challenging.
- $b\tau(\text{lep})\nu bW(\text{had})$ : This channel is characterized by a single isolated lepton and large missing  $E_T$  due to the neutrinos in the final state which make a full kinematic reconstruct of the event impossible. The presence of a signal could be detected via the excess of kinematically  $\tau$ -like events or it could be inferred from an analysis of the ‘generalized transverse mass’ spectrum [11].
- $b\tau(\text{had})\nu bW(\text{lep})$ : As above, due to the large number of neutrinos in the final state, a full kinematic reconstruction of the event will not be possible and a potential signal is again recognized by an excess of kinematically  $\tau$  like events.

The most sensitive channel for a discovery of a light charged Higgs boson is that where both the  $\tau$  and the  $W$  decay hadronically.

### 1.3.2. Heavy Charged Higgs Boson Searches: $m_{H^\pm} > m_t$

For the search for a heavy charged Higgs boson, two channels are considered:

- $bq[b\tau(\text{had})\nu$ : This channel is characterized by one hard  $\tau$  jet from the decay of the charged Higgs boson, large missing transverse momentum, one or two  $b$  jets, and two light jets.
- $b\ell\nu[b]bqqb$ : Here, the charged Higgs boson decays into a  $tb$  final state. In addition 3 – 4  $b$ -jets are expected in the event (depending on the production mechanism), 2 light quark jets, and one high  $p_T$  lepton.

Of these two channels, only the first one shows a sensitivity to charged Higgs boson production.

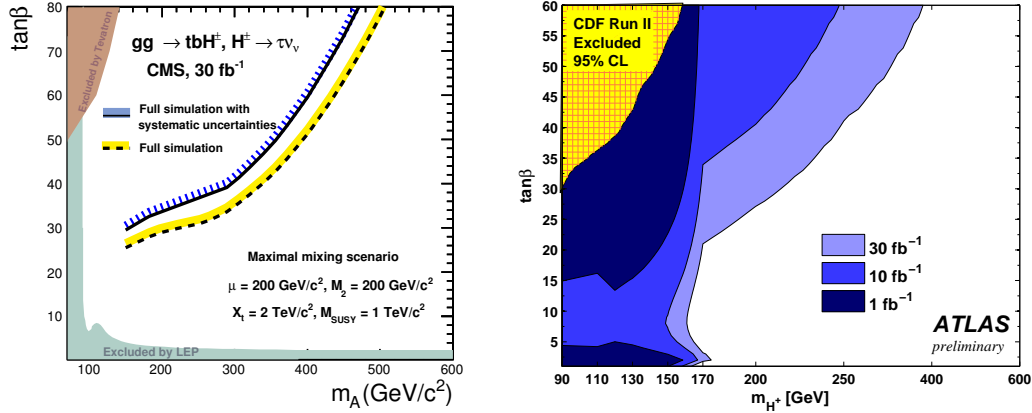


Figure 8: Left: Discovery potential for a charged Higgs boson as a function of  $m_A$  and  $\tan\beta$  for an integrated luminosity of 30 fb<sup>-1</sup> (CMS). Right: Discovery potential for a charged Higgs boson as a function of  $m_{H^\pm}$  and  $\tan\beta$  for integrated luminosities between (1 – 30) fb<sup>-1</sup> (ATLAS). In addition, the 95% exclusion limit from CDF (Run-II) is shown.

### 1.3.3. Overall Discovery Potential for Charged Higgs Bosons

In Figure 8 the overall discovery potential is displayed for CMS (left) [4] and ATLAS<sup>1</sup> [5] (right). The range of low charged Higgs boson masses up to the top quark mass is well covered, and a charged Higgs boson can be discovered with a data set corresponding to an integrated luminosity of 30 fb<sup>-1</sup>. For charged Higgs boson masses above the top quark mass, high values of  $\tan\beta$  would be necessary for a 5 $\sigma$  discovery.

## 2. MEASUREMENT OF HIGGS BOSON PROPERTIES

Once the Higgs boson has been discovered at the LHC, the measurement of its properties like mass, spin, CP eigenvalue and its couplings to fermions and gauge bosons would have to be measured in order to obtain further insight into the mass generation mechanism realized in nature.

### 2.1. The Higgs Boson Width

In addition to a potential Higgs boson discovery in the  $h/H/A \rightarrow \mu\mu$  channel, due to its excellent mass resolution, the width of the Higgs boson and therefore  $\tan\beta$  can be directly measured [4]. In Figure 9 (left) the intrinsic width of the Higgs boson (circles) and that measured (solid triangles) for  $m_A = 150$  GeV is shown. In such an analysis it has to be taken into account that the mass degeneracy of the neutral Higgs bosons  $A$  and  $H$  is not exact which is illustrated by the open triangles. This is particularly evident for  $m_A = 150$  GeV and low  $\tan\beta$  where the mass difference is larger than the intrinsic width. In Figure 9 (right) the expected uncertainty (including a theoretical uncertainty of 15%) of the  $\tan\beta$  measurement is shown as a function of  $m_A$  and  $\tan\beta$ . The measurement of  $\tan\beta$  can be further constrained by cross section measurements since  $\sigma \times \text{BR} \sim \tan\beta_{\text{eff}}$ .

### 2.2. The Higgs Boson Mass

In the SM, the mass of the Higgs boson can be measured with the highest precision in the decay channels  $H \rightarrow ZZ^{(*)} \rightarrow 4\ell$ , in  $H \rightarrow \gamma\gamma$ , and in  $H \rightarrow b\bar{b}$  [12]. However, recent studies indicate that a discovery of the Higgs

<sup>1</sup>Here, a statistical uncertainty corresponding to that expected for the integrated luminosities given is assumed.

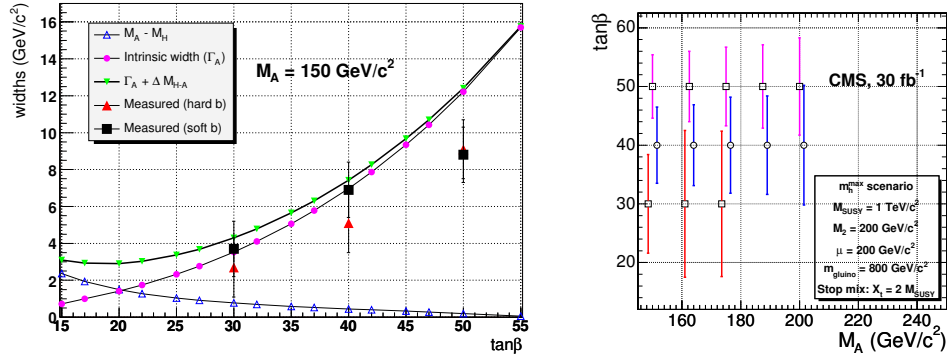


Figure 9: Left: The comparison between the expected Higgs boson width and the measured width as a function of  $\tan\beta$  for  $m_A = 150$  GeV. Right: Uncertainty on the  $\tan\beta$  measurement obtained from the Higgs boson width measurement with an integrated luminosity of  $30 \text{ fb}^{-1}$ .

boson in the  $b\bar{b}$  and therefore a measurement of its mass might be challenging [5]. Assuming  $300 \text{ fb}^{-1}$  of data, a relative precision of such a measurement of 0.1% in the range  $100 < m_H < 400$  GeV can be achieved as displayed in Figure 10 (left). The anticipated precision degrades down to 1% for Higgs boson masses of  $m_H = 700$  GeV. The systematic uncertainties are dominated by the knowledge of the absolute calorimetric energy scale which, for leptons and photons, was assumed to be 0.1%. However, a final value of 0.02% for that uncertainty is anticipated driven by the objective to measure the mass of the  $W$  boson with a precision of 15 MeV. An uncertainty of 1% on the jet energy scale was assumed.

In models beyond the SM (like the MSSM), the coupling of the Higgs boson to gauge bosons might be suppressed or even absent. In that case the mass of the Higgs boson can be measured, e.g. in the  $H \rightarrow b\bar{b}$ ,  $H \rightarrow \mu\mu$  or  $H \rightarrow \tau\tau$  channel. In the latter case, due to the neutrinos from the  $\tau$  decays, one would have to use techniques like the collinear approximation to reconstruct the mass of the Higgs boson. In all cases, a precision on the % level or better can be expected.

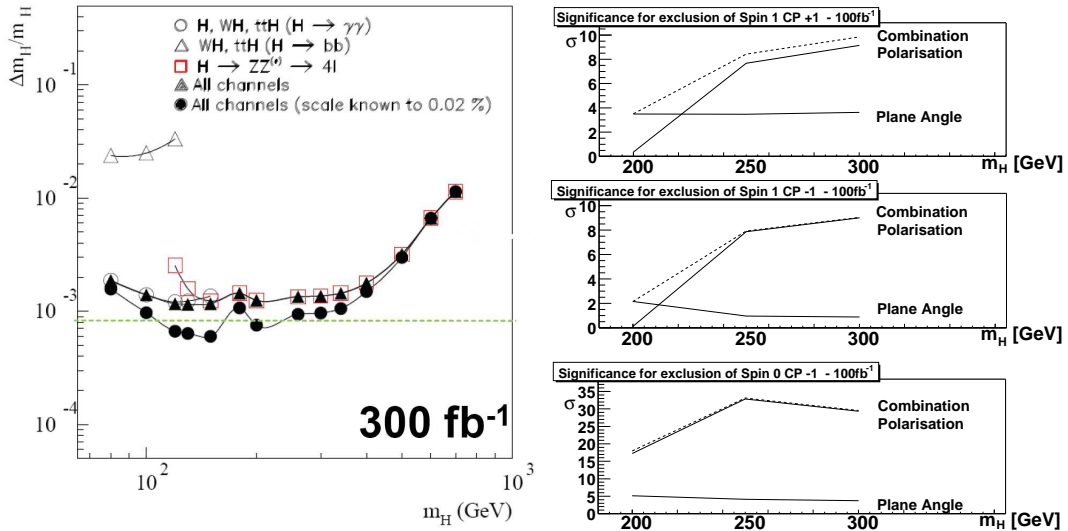


Figure 10: Left: The anticipated precision of a measurement of the Higgs boson mass in the decay channels  $H \rightarrow \gamma\gamma$  (open circles),  $H \rightarrow b\bar{b}$  (open triangles), and  $H \rightarrow ZZ^{(*)} \rightarrow 4l$  (rectangles). A precision of the order of 0.1% can be achieved for Higgs boson masses of  $100 < m_H < 400$  GeV, while for  $m_H = 700$  GeV 1% is expected in  $300 \text{ fb}^{-1}$  of data. Right: The significance for the exclusion of a Higgs boson with non-SM like spin and CP eigenvalues as a function of its mass.



### 2.3. Spin and CP of the Higgs Boson

After the discovery of the Higgs boson, the highest priority is to establish its spin and CP eigenvalue. This can be determined from a study of the angular distributions and correlations in the  $H \rightarrow ZZ(*) \rightarrow 4\ell$  channel [13, 14]. The angular distributions investigated are the polar angle of the leptons relative to the direction of flight of the  $Z$  boson, and the angle between the decay planes of the two  $Z$  bosons, both calculated in the Higgs boson rest frame.

The result of this study is shown in Figure 10 (right) for non-SM like spin and CP configurations for the Higgs boson. For masses larger than 230 GeV a spin-1 hypotheses with either even or odd CP eigenvalue can be ruled out with a data set of  $100 \text{ fb}^{-1}$ . For masses as low as 200 GeV and a luminosity of  $300 \text{ fb}^{-1}$ , a Higgs boson with (spin, CP)=(1,+) can be ruled out at the  $6.4 \sigma$  level, while for (spin, CP)=(1,-) a significance of only  $3.9 \sigma$  can be obtained. A Higgs boson with (spin, CP)=(0,-) can be ruled out with less than  $100 \text{ fb}^{-1}$  over the whole mass range considered here.

### 2.4. The Higgs Boson Couplings

The coupling of the Higgs boson to gauge bosons and fermions determines its production cross section and branching fractions. Measuring the rates in multiple channels allows for a determination of various combinations of couplings at the LHC [15]. However, a model independent measurement of the (partial) decay width(s) of the Higgs boson will not be possible at the LHC. The reason being that on the one hand a measurement of the missing mass spectrum like at  $e^+e^-$  colliders is not possible, and that on the other hand some of the decay channels of the Higgs boson are either hard (like  $H \rightarrow b\bar{b}$ ) or even impossible (like  $H \rightarrow gg$ ) to detect due to the overwhelming background from QCD processes. An absolute measurement of the above quantities will only be possible if additional theoretical assumptions are being made. Introducing moderate theoretical constraints as detailed below, allows to overcome the experimental difficulties described above and to measure the couplings of the Higgs boson.

In a first approach, only the couplings of the Higgs boson to the gauge bosons is constrained to less than 1.05 times its value in the  $\text{SM}^2$ , which is justified in any model with an arbitrary number of Higgs doublets. Furthermore,

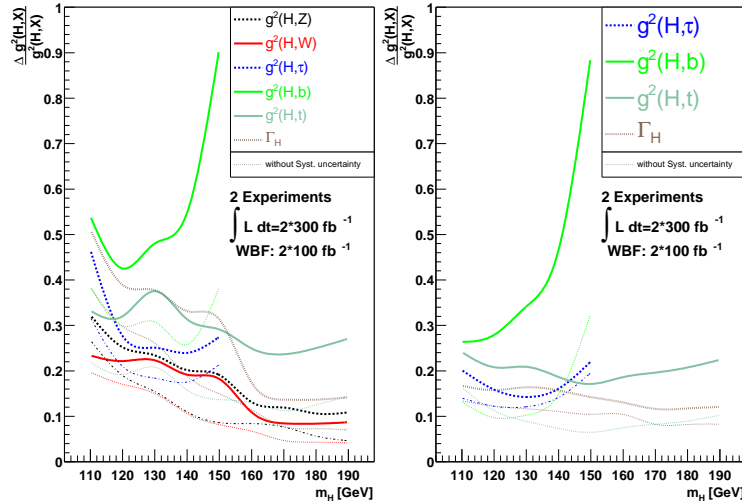


Figure 11: Relative precision of a measurement of the Higgs boson couplings squared as a function of  $m_H$  for an integrated luminosity of  $300 \text{ fb}^{-1}$  per experiment with moderate (left) and more restrictive (right) theoretical assumptions as explained in the text.

<sup>2</sup>The additional 5% account for theoretical uncertainties in the translation between the couplings squared and the partial widths, and also for small possible admixtures of exotic Higgs states.

additional particles running in loops in the  $H \rightarrow \gamma\gamma$  and  $gg \rightarrow H$  processes are allowed. The relative precision of the measured couplings as a function of the Higgs boson mass is illustrated in Figure 11 (left) assuming an integrated luminosity of  $300 \text{ fb}^{-1}$  per experiment. The couplings of the Higgs boson to the  $W$  and  $Z$  bosons, to the top quark, and to the  $\tau$  lepton can be measured with a precision between (10 – 40)% depending on  $m_H$ .

If in addition, the ratio of the  $W$  and  $Z$  couplings to the Higgs boson are constrained to within 1% of that in the SM, the absolute value of the  $W$  coupling to within 5%, and no new non-SM particles are allowed in the loops, a higher precision can be obtained as illustrated in Figure 11 (right). In that case a precision of the measurement of the couplings squared can be achieved which is about a factor of two higher.

### 3. SUMMARY

In this note, the discovery potential for neutral ( $h/H/A$ ) and charged ( $H^\pm$ ) Higgs bosons in the MSSM in ATLAS and CMS at the LHC has been reviewed. After a potential discovery of a Higgs boson, its properties have to be measured in order to gain insight into the mass generation mechanism realized in nature. Possible measurements of the Higgs boson mass and width, its spin and CP eigenvalue, and its couplings to fermions and gauge bosons have been discussed.

### Acknowledgments

The author wishes to thank the organizers of the conference for the invitation and everybody in the ATLAS and CMS Higgs working groups that helped in preparing the talk.

### References

- [1] M. S. Carena, S. Heinemeyer, C. E. M. Wagner and G. Weiglein, *Eur. Phys. J. C* **26** (2003) 601.
- [2] The ATLAS Collaboration, G. Aad et al., “The ATLAS Experiment at the CERN Large Hadron Collider”, *JINST* **3** (2008) S08003.
- [3] The CMS Collaboration, S. Chatrchyan et al, “The CMS experiment at the CERN LHC”, *JINST* **3** (2008) S08004.
- [4] The CMS Collaboration, G. L. Bayatian *et al.*, *J. Phys. G* **34** (2007) 995.
- [5] ATLAS Collaboration, Expected Performance of the ATLAS Experiment, Detector, Trigger and Physics, CERN-OPEN-2008-020, Geneva, 2008, to appear.
- [6] S. Lehti, “Study of  $H/A \rightarrow \tau\tau \rightarrow e\mu + X$  in CMS”, CMS Note 2006/101 (2006).
- [7] R. K. Ellis, I. Hinchliffe, M. Soldate and J. J. van der Bij, *Nucl. Phys. B* **297** (1988) 221.
- [8] R. Kunnunen, and S. Lehti, “Search for the Heavy Neutral MSSM Higgs Boson with the  $H/A \rightarrow \tau\tau \rightarrow$  Electron plus Jet Decay Mode”, CMS Note 2006/075 (2006).
- [9] A. Kalinowski, M. Konecki, and D. Kotlinski, “Search for MSSM heavy neutral Higgs boson in  $\tau + \tau \rightarrow \mu +$  jet Decay Mode”, CMS Note 2006/105 (2006).
- [10] S. Genai, A. Nikitenko, and L. Wendland, “Search for MSSM Heavy Neutral Higgs Boson in  $\tau\tau \rightarrow$  two Jet Decay Mode”, CMS Note 2006/126 (2006).
- [11] E. Gross and O. Vitells, arXiv:0801.1459 [physics.data-an].
- [12] ATLAS Collaboration, “Detector and Physics Performance Technical Design Report”, CERN-LHCC/99-14/15 (1999).
- [13] C. P. Buszello, I. Fleck, P. Marquard and J. J. van der Bij, *Eur. Phys. J. C* **32**, 209 (2004).
- [14] M. Bluj, “A Study of Angular Correlations in  $H \rightarrow ZZ \rightarrow 2e2\mu$ ”, CMS Note 2006/094.
- [15] M. Duhrssen, S. Heinemeyer, H. Logan, D. Rainwater, G. Weiglein and D. Zeppenfeld, *Phys. Rev. D* **70** (2004) 113009.